


## Research Paper

# Gut-brain axis metabolic pathway regulates antidepressant efficacy of albiflorin

Zhen-Xiong Zhao<sup>1\*</sup>, Jie Fu<sup>1\*</sup>, Shu-Rong Ma<sup>1\*</sup>, Ran Peng<sup>1</sup>, Jin-Bo Yu<sup>1</sup>, Lin Cong<sup>1</sup>, Li-Bin Pan<sup>1</sup>, Zuo-Guang Zhang<sup>2</sup>, Hui Tian<sup>2</sup>, Chun-Tao Che<sup>3</sup>, Yan Wang<sup>1</sup>, Jian-Dong Jiang<sup>1</sup>

1. State Key Laboratory of Bioactive Substance and Function of Natural Medicines, Institute of Materia Medica, Chinese Academy of Medical Sciences / Peking Union Medical College, Beijing 100050, China
2. Beijing WONNER Biotech. Co. Ltd, Beijing 100071, China
3. College of Pharmacy, The University of Illinois at Chicago, Chicago 60607, United States

\*These authors made an equal contribution to this work.

 Corresponding authors: Dr. Yan Wang, Tel.: +86 10 63165238; fax, +86 10 63165238, e-mail address: wangyan@imm.ac.cn; or Dr. Jian-Dong Jiang, Tel.: +86 1083160005; fax, +86 10 63017757, e-mail address: jiang.jdong@163.com

© Ivyspring International Publisher. This is an open access article distributed under the terms of the Creative Commons Attribution (CC BY-NC) license (<https://creativecommons.org/licenses/by-nc/4.0/>). See <http://ivyspring.com/terms> for full terms and conditions.

Received: 2018.06.23; Accepted: 2018.10.08; Published: 2018.11.13

## Abstract

The gut microbiota is increasingly recognized to influence brain function through the gut-brain axis. Albiflorin, an antidepressant natural drug in China with a good safety profile, is difficult to absorb and cannot be detected in the brain after oral administration. Accordingly, the antidepressant mechanism of albiflorin *in vivo* has not been elucidated clearly.

**Methods:** We identified benzoic acid as the characteristic metabolite of albiflorin *in vivo* and *in vitro*, then discovered the roles of gut microbiota in the conversion of albiflorin by carboxylesterase. Pharmacodynamic and pharmacokinetic studies were performed for the antidepressant activities of albiflorin in animals, and the efficacy of benzoic acid in inhibiting D-amino acid oxidase (DAAO) in brain was further investigated.

**Results:** We validated that gut microbiota transformed albiflorin to benzoic acid, a key metabolite in the intestine that could cross the blood-brain barrier and, as an inhibitor of DAAO in the brain, improved brain function and exerted antidepressant activity *in vivo*. Intestinal carboxylesterase was the crucial enzyme that generated benzoic acid from albiflorin. Additionally, the regulatory effect of albiflorin on the gut microbiota composition was beneficial to alleviate depression.

**Conclusion:** Our findings suggest a novel gut-brain dialogue through intestinal benzoic acid for the treatment of depression and reveal that the gut microbiota may play a causal role in the pathogenesis and treatment of the central nervous system disease.

Key words: gut-brain axis, albiflorin, gut microbiota, depression, benzoic acid, carboxylesterase

## Introduction

Depression is a common disorder that is characterized by a persistent low mood. As a prevalent psychiatric disorder, it affects 21% of the global population [1]. However, depression is widely undiagnosed and untreated because of the associated stigma, lack of effective therapies, and inadequate mental health resources [2]. Neurotransmitter deficiencies [3], neurotrophic alterations [4], endocrine-immune system dysfunction [5], and

neuroanatomical abnormalities [6] have been shown to be related to depression. The antidepressants currently in use include tricyclic antidepressants, selective serotonin reuptake inhibitors (SSRIs), monoamine oxidase inhibitors, and serotonin (5-HT) and norepinephrine (NE) reuptake inhibitors [7, 8]. Most antidepressants have a certain level of toxicity and side effects [7, 9]; thus, studies aiming to identify new antidepressants with good efficacy and low

toxicity are critical.

The gut microbiota is considered a “hidden organ” in the body and may be associated with the pathogenesis of various diseases, such as cardiovascular diseases, diabetes, and obesity [10-15]. In particular, recent research has proposed a new concept, called the “gut-brain axis”, which has opened up new possibilities for the treatment of central nervous system diseases [16, 17]. Some studies have shown that the gut microbiota is closely related to the onset and treatment of depression [18-20]. Because natural drugs with low bioavailability unavoidably interact with the intestinal bacteria after oral administration, gut microbiota would represent a potential new strategy to study the mechanism of drug efficacy [21-23].

*Paeoniae Radix Alba*, known as the root of white peony, has pharmacological activities including alleviating pain, tonifying blood, and regulating menstruation [24]. It was widely used in Chinese herbal formulas with a long history of good safety [25], such as Xiaoyao-wan and Xiaoyao-san prescribed for the treatment of depression-like disorders [26-28]. Albiflorin, a major monoterpene glycoside isolated from *Radix Paeoniae Alba*, showed more significant antidepressant activity than its isomer paeoniflorin in *Paeonia lactiflora* [29].

Post-traumatic stress disorder is a severe psychiatric disorder. Behavioral deficits related to this disorder observed in rats subjected to a single prolonged stressful experience were reversed by albiflorin [30]. Research on the antidepressant mechanism of albiflorin in the central nervous system has shown that the levels of tyrosine hydroxylase, dopamine D2 receptor, and dopamine transporter in the hypothalamus were normalized after treatment with albiflorin in rats subjected to chronic unpredictable mild stress [31]. Albiflorin also up-regulated levels of hippocampal brain-derived neurotrophic factor, 5-hydroxytryptamine, and 5-hydroxyindoleacetic acid [29]. Furthermore, albiflorin increased the extracellular concentrations of noradrenaline and 5-hydroxytryptamine in the hypothalamus of freely moving rats [32].

However, as a natural product, albiflorin was observed at low concentrations in the blood and brain after oral administration [33]. Because of these obstacles, the therapeutic molecules of the antidepressant albiflorin *in vivo* have not been completely elucidated. Indeed, low bioavailability is a common problem of many effective natural compounds. In the present study, we have identified a characteristic albiflorin metabolite, benzoic acid, transformed by the gut microbiota. After crossing the blood-brain barrier (BBB), benzoic acid enters the

central nervous system to cause antidepressant effects. Our work reveals that the gut microbiota structure might play a key role in the treatment of this central nervous system disease.

## Methods

### Chemicals and reagents

Albiflorin was provided by WONNER Biotech. Co. Ltd. (Beijing, China). Benzoic acid was purchased from the National Institutes for Food and Drug Control (Beijing, China). The purity of the compounds was higher than 98% (HPLC). HPLC-grade acetonitrile, methanol, and ammonia were purchased from Fisher Scientific (Fair Lawn, NJ, USA). The carboxylesterase inhibitor bis-p-nitrophenyl phosphate (BNPP) and fluoxetine (FXT) were obtained from Solarbio Life Sciences Co., Ltd. (Beijing, China). Reserpine and the D-amino acid oxidase inhibitor AS057278 were purchased from J&K Scientific, Ltd. (Beijing, China). D-amino acid oxidase was obtained from Sigma-Aldrich (NJ, USA). Mice D-amino acid oxidase and carboxylesterase ELISA kits were purchased from Shanghai Jianglai Biotechnology Co., Ltd (Shanghai, China).

### Instruments

An HPLC-MS/MS 8050 system from Shimadzu Corporation (Kyoto, Japan) was used to determine the concentrations of albiflorin and benzoic acid. Chromatographic separation of the analytes was achieved on a Shim-pack ODS-II column (2.2  $\mu\text{m} \times 2 \text{ mm} \times 75 \text{ mm}$ , Shimadzu Corporation, Kyoto, Japan), and the column temperature was maintained at 40 °C. Linear gradient elution was performed at a flow rate of 0.4 mL/min with water and ammonia (99.95: 0.05, v/v) as mobile phase A and methanol as mobile phase B: 0.00 min (80% A and 20% B), 1 min (80% A and 20% B), 1.01 min (60% A and 40% B), 3 min (20% A and 80% B), 3.01 min (80% A and 20% B) and 5 min (80% A and 20% B) for 8 min. The autosampler temperature was set to 4 °C. The mass spectrometer was run in the multiple reaction monitoring (MRM) mode. The following precursors to product ions were monitored: 503.33 [M+Na]<sup>+</sup>  $\rightarrow$  341.05 for albiflorin (*m/z*), 121.10 [M-H]<sup>-</sup>  $\rightarrow$  77.10 for benzoic acid. The nebulizing gas, drying gas, and heating gas flow rates were 3 L/min, 10 L/min, and 10 L/min, respectively.

### Animals

Male Sprague-Dawley (SD) rats (180–200 g) and ICR mice (18–22 g) were supplied by the Institute of Laboratory Animal Science, Chinese Academy Medical Sciences (Beijing, China). Animals were housed in cages placed in racks in a room with a 12-h light/dark cycle (lights on from 8: 00 AM to 8: 00 PM)

a temperature of (22–24 °C) and 45% relative humidity. Rats were fasted for 12 h before the experiments, but otherwise had free access to food and water. The study was conducted in accordance with institutional guidelines and ethics and was approved by the Laboratories Institutional Animal Care and Use Committee of the Chinese Academy of Medical Sciences and Peking Union Medical College.

### Identification of albiflorin metabolites *in vivo*

LC/MS<sup>n</sup>-IT-TOF (Shimadzu, Tokyo, Japan), was used to identify the metabolites of albiflorin in the feces. Chromatographic separation of the analytes was achieved on Altima C<sub>18</sub> (250 mm × 4.6 mm × 5 μm). Linear gradient elution was performed at a flow rate of 0.8 mL/min with water/ 0.5% formic acid as mobile phase A, and methanol as mobile phase B: 0.00 min (90% A and 5% B), 10 min (90% A and 5% B), 30 min (55% A and 25% B), 40 min (25% A and 75% B) and 40.01 min (90% A and 10% B) for 45 min. The autosampler temperature was set at 4 °C. The nebulizing gas: 1.5 L/min, CDL temperature: 200 °C, heat block temperature: 200 °C, detector voltage: 1.75 kV, collision energy: 50%. Before LC/MS<sup>n</sup>-IT-TOF analysis, the feces were extracted with methanol (1/10, g/mL) by ultrasound for 30 min. Subsequently, they were centrifuged for 10 min at 21100 ×g. Finally, 20 μL of the supernatant was injected for LC/MS<sup>n</sup>-IT-TOF.

### Albiflorin metabolized by the gut microbiota *in vitro*

Colon contents from six SD rats were pooled, and 5 g of the sample was transferred to a flask containing an anaerobic medium (100 mL). After thorough mixing, cultures (containing the gut microbiota and anaerobic medium) were pre-incubated under anaerobic conditions with an N<sub>2</sub> atmosphere at 37 °C for 60 min. Next, 100 μL of albiflorin was added to the fresh rat gut microbiota cultures (900 μL), with water (100 μL) as the negative control. The final concentration of albiflorin in the incubation system was 1 mg/mL. Cultures were incubated at 37 °C for 0, 2, 6, 12, or 24 h. The method was similar to a previously described procedure [34]. The carboxylesterase inhibitor BNPP (0.3, 0.9, and 3 mM) was added to the incubation system at the same time.

Alb and its metabolites were separated by an Altima C<sub>18</sub> column (250 × 4.6 mm, 5 μm). The mobile phase consisted of (A) 0.1% glacial acetic acid in water and (B) acetonitrile with a gradient elution as follows: 10% eluent B for 5 min, 10%-45% eluent B from 10 to 30 min, 45%-75% eluent B from 30 to 40 min, 75%-85% eluent B from 40 to 55 min, back to 10% eluent B at

55.01 min and maintained for 5 min for column equilibration. The flow rate and the column temperature were 0.8 mL/min and 35 °C, respectively. For IT-TOF analysis, both positive and negative ESI were used to detect the samples. Nitrogen was used as the nebulizing gas, and helium was used for MS<sup>n</sup> analytic fragmentations. Other parameters were as follows: CDL temperature, 200 °C; heat block temperature, 200 °C; detector voltage, 1.70 kV; nebulizing gas, 1.5 L/min; drying gas pressure, 110 kPa. The energy of CID was set at 50%. Mass spectra were acquired in the range of m/z 100-1000 for MS<sup>1</sup>. The MS<sup>n</sup> data were collected in automatic mode.

### Albiflorin metabolized by 18 bacterial strains *in vitro*

Eighteen strains of the gut microbiota, *Enterobacter aerogenes*, *Enterococcus faecium*, *Escherichia coli*, *Klebsiella pneumoniae*, *Pseudomonas aeruginosa*, *Proteus vulgaris*, *Bacteroides fragilis*, *Peptostreptococcus anaerobius*, *Clostridium butyricum*, *Lactobacillus casei*, *Lactobacillus acidophilus*, *Bifidobacterium longum*, *Proteus mirabilis*, *Enterobacter cloacae*, *Staphylococcus epidermidis*, *Enterococcus faecalis*, *Staphylococcus aureus* and *Bifidobacterium breve*, were purchased from Nanjing Bianzhen Biotechnology Co. Ltd. After activating the strains, the method described above was used to measure the metabolites of albiflorin. Carboxylesterase levels were detected using the carboxylesterase ELISA kit purchased from Solarbio Life Sciences Co., Ltd. (Beijing, China), according to the manufacturer's guidelines. The genes encoding carboxylesterases of *S. aureus* ATCC 6538 (four genes), *E. faecalis* ATCC 29212 (two genes) and *B. breve* ATCC 15700 (four genes) were PCR amplified. The sequences of these genes were identified and verified by agarose gel electrophoresis and sequencing. DNA enzymes were used according to the manufacturers' recommendations. All fragments were validated by Sanger 3730 sequencing.

### Molecular docking between albiflorin and carboxylesterase

Discovery Studio Client software (v16.1.0.15350) was used to compute the possible interaction of albiflorin with carboxylesterase, whose crystal structures are available in the Protein Data Bank. CDOCKER was used to analyze the binding between hit compounds and the protein. The pose cluster radius was set to 0.5, and the other docking parameters were all set to the default values.

### Carboxylesterase-mediated conversion of albiflorin to benzoic acid

Liver and gut microbiota were taken from three SD rats and the liver homogenate was prepared with saline 1:4 (v/v). The activity of carboxylesterase was detected using carboxylesterase ELISA kit. At the same time, albiflorin was added to the liver homogenate or the gut microbiota, and the albiflorin final concentration was set at 0.25 mg/mL. After incubating at 37 °C for 1 h, 100 µL of the homogenate was taken, and 200 µL of methanol was added. Subsequently, 10 µL of the supernatant was filtered and used for HPLC analysis after centrifugation for 10 min at 21100 ×g.

### Inhibition of D-amino acid oxidase (DAAO) by benzoic acid in the brain *in vitro*

D-serine (final concentration 200 µg/mL) was used as the substrate probe in the oxidation reaction and was incubated with DAAO (0.05 mg/mL) *in vitro*. AS057278 (89 µM), the known inhibitor of DAAO, was applied to verify the effects of benzoic acid (89 µM) and albiflorin (223 µM) in the incubation system with DAAO enzyme. After 15 min incubation at 37 °C, the percentage of D-serine in DAAO system was detected by LC-MS/MS.

Ten ICR mice were sacrificed by cervical dislocation for the collection of brains, which were washed with saline and dried by filter papers. After weighing, the brains were homogenized with 2 times volumes [v (mL)/w (g)] of saline. Benzoic acid (final concentrations of 5 µg/mL or 10 µg/mL) was added to the brain homogenate and incubated for 30 min at 37 °C. Also, albiflorin (final concentration of 10 µg/mL) was added to the homogenate. The activity of DAAO was determined using a DAAO ELISA kit (Shanghai Jianglai Biotechnology Co., Ltd, China.).

### Pseudo-germ-free (PGF) mice and pharmacokinetic study *in vivo*

Sixty-six ICR mice were orally administered cefadroxil (100 mg/kg), terramycin (300 mg/kg), and erythromycin (300 mg/kg) twice a day for 3 days. Another 36 ICR mice were orally administered an equivalent volume of saline. Pharmacokinetic examinations were performed 2 days after the final administration. Mouse feces were collected on the third day after the final treatment with antibiotics, and germ-free status was confirmed by culturing fecal samples aerobically on a nutrient agar culture medium. Fecal samples from rats that were not treated with antibiotics served as control samples.

Before the oral administration of a single dose of albiflorin (14 mg/kg), the PGF mice were fasted overnight with free access to water. Blood samples

were collected before and at 0.08, 0.17, 0.33, 0.5, 0.75, 1, 1.5, 2, 4, 8, and 10 h after drug treatment. Fecal samples were also collected at 0, 6, 12, 24, and 48 h after albiflorin treatment. Brains were removed at 0, 1, 2, 6, and 8 h.

Three groups of ICR mice (n=6/group) were given albiflorin orally at 3.5, 7, or 14 mg/kg. The fourth group of ICR mice (n=6) was given albiflorin (1.75 mg/kg) by intravenous administration. Blood samples were collected before and at 5 min, 10 min, 20 min, 30 min, 45 min, 1 h, 1.5 h, 2 h, 3 h, 4 h, 6 h, and 8 h after drug treatment.

### Antidepressant activity of albiflorin

Sixty SD rats were used to establish a chronic stress-induced depression model through the administration of multiple alternating stimuli for 8 weeks. The animals were randomly divided into 6 groups (n=10). Ten rats were normally bred and not stimulated, as group 1 (normal control group); group 2 was the untreated model control group; group 3 included model rats treated with benzoic acid (14 mg/kg); group 4 included model rats treated with albiflorin (7 mg/kg); group 5 included model rats treated with albiflorin (14 mg/kg); group 6 included PGF rats treated with albiflorin (14 mg/kg). The PGF rats were continuously on antibiotic treatment during the 14-day Alb treatment. The sugar preference tests were performed on days 0 and 14 of treatment. After a 2-week treatment, feces samples were collected for 16S rRNA gene analysis, and brains were also removed for albiflorin detection.

Forty ICR mice were used in a forced swimming test. Animals were randomly divided into 4 groups (n=10). One day before treatment, all mice were forced to swim for 15 min in a training session. Group 1 was the untreated control group, group 2 was treated with albiflorin (7 mg/kg), group 3 was treated with albiflorin (14 mg/kg), and group 4 included PGF mice treated with albiflorin (14 mg/kg). Two hours after treatment, ICR mice were forced to swim for 5 min. Immobility time in the last 3 min was recorded.

Eighty ICR mice were randomly divided into 8 groups to perform a reserpine-induced acute depression model [35] as follows: normal control group (Group 1), reserpine-induced model group (Group 2), low-dose albiflorin group (7 mg/kg, Group 3), high-dose albiflorin group (14 mg/kg, Group 4), combined antibiotics-treated group (Group 5), albiflorin-treated PGF group (14 mg/kg, Group 6), benzoic acid group (14 mg/kg, Group 7), and fluoxetine group (10 mg/kg, Group 8). Mice were orally administrated as described above for 7 consecutive days (except mice in Group 2 who were treated with saline). After the final drug



administration, mice were injected intraperitoneally with 4 mg/kg reserpine except for Group 1. The degree of ptosis was recorded at 1 h after the reserpine injection according to the following rating rule: 0, eyes open; 1, one-quarter closed; 2, half closed; 3, three-quarters closed; 4, completely closed [36]. Then, each mouse was placed in the center of a circle with a radius of 7.5 cm, and the out-circle rate was recorded in 15 s. Tail suspension test was carried out 1.5 h after reserpine injection, and immobility was determined for the last 4 min of a 6 min test [36]. Body temperatures were measured 4 h after the reserpine injection.

### Bacterial composition analysis

16S rRNA genes were amplified using specific primers targeting the 16S V3-V4 regions named 340F-805R. The methods were the same as those used in our previous study [37]. Sequences with  $\geq$  equisimilarity values were assigned to the same OTUs.

### Statistical analysis

Statistical analyses were conducted using two-way ANOVA and Student's t-test with GraphPad Prism Version 5 (GraphPad Software, CA, USA). Data are expressed as mean  $\pm$  standard deviation, and *P* values less than 0.05 were considered statistically significant.

## Results

### Identification of albiflorin metabolites *in vivo* and *in vitro*

Metabolites in the feces of ICR mice were identified by LC/MS<sup>n</sup>-IT-TOF. Four metabolites (**Figure 1**) were detected in the feces samples collected after albiflorin administration to mice (**Figure 2A**), including two phase I (M1, M2) and two phase II (M3, M4) metabolites, which were absent or present in negligible amounts in the blank samples. MS<sup>1</sup> and multistage mass spectrometry information are shown in **Table 1**. The [M+H]<sup>+</sup> of the parent drug albiflorin was at *m/z* 481.1772; the mass spectral data of the parent drug and metabolites are listed in **Table 1**. The phase I metabolite, M1 (hydroxylalbiflorin), was eluted at 13.6 min, which showed an [M+H]<sup>+</sup> peak at *m/z* 497.1907, 16 Da more than that of albiflorin. MS<sup>2</sup> and MS<sup>3</sup> fragment ions were both 16 Da more than the parent drug. M1 was presumed to be the hydroxylated metabolite of albiflorin with a mass gain of 16. M2 (dihydroxylalbiflorin) was eluted at 4.7 min and showed an [M+H]<sup>+</sup> peak at *m/z* 513.2050 and was 32 Da more than that of albiflorin. MS<sup>2</sup> and MS<sup>3</sup> fragment ions, *m/z* 215.1273  $\rightarrow$  197.0932 (18 Da, loss of H<sub>2</sub>O) and 215.1273  $\rightarrow$  179.0973 (36 Da, loss of 2 H<sub>2</sub>O)

indicated that there were two hydroxyl groups in the fragments. Based on the above results, M2 was identified as the dihydroxylated metabolite of albiflorin with a mass gain of 32. The phase II metabolite, M3 had a retention time of 21.7 min with a [M+H]<sup>+</sup> peak at *m/z* 643.2532 and [M+Na]<sup>+</sup> peak at *m/z* 664.2336, 162 Da more than that of albiflorin. MS<sup>2</sup> fragment ions were at *m/z* 503.1720 and 481.1702. They were the same as the [M+H]<sup>+</sup> and [M+Na]<sup>+</sup> peaks of albiflorin, indicating that M3 was a metabolite of albiflorin. Based on the above results, M3 was identified as glucuronic acid-conjugated albiflorin. The phase II metabolite, M4, eluted at 24.1 min, showed an [M-H]<sup>-</sup> ion at *m/z* 784.2860, which was 305 Da more than that of albiflorin. MS<sup>2</sup> fragment ions were at *m/z* 479.1536, which indicated that M4 was a metabolite of albiflorin. Combining its [M-H]<sup>-</sup> ion, M4 might be a metabolite of albiflorin binding with glutathione (glutathione-conjugated albiflorin). These four metabolites had low concentrations in feces and were not detected in blood. Natural compounds with low bioavailability might interact with intestinal bacteria; therefore, we focused our attention on the bio-transformation of albiflorin in the gut microbiota.

**Table 1.** Multistage mass spectrometry results of albiflorin and its metabolites.

	ESI	MS <sup>1</sup> <i>m/z</i>	Fragments	
			MS <sup>2</sup> <i>m/z</i>	MS <sup>3</sup> <i>m/z</i>
Albiflorin	+	481.1772 [M+H] <sup>+</sup> 503.1874 [M+Na] <sup>+</sup>	197.0816	179.0708
M1	+	497.1907 [M+H] <sup>+</sup>	215.1273	197.0932 179.0973
M2	+	513.2050 [M+H] <sup>+</sup>	233.1904	215.1642 197.1093 179.1046
M3	+	643.2532 [M+H] <sup>+</sup> 664.2336 [M+Na] <sup>+</sup>	481.1702 503.1720	197.1034 179.1022
M4	-	784.2860 [M-H] <sup>-</sup>	479.1536	-
BA	-	121.0304 [M-H] <sup>-</sup>	-	-

SD rat intestinal bacteria were collected for an *in vitro* anaerobic incubation in the presence of albiflorin. As shown in **Figure 2C-D**, after a 12 h incubation with the intestinal bacteria, albiflorin (retention time 15.4 min) was completely transformed into a new metabolite (retention time 21.6 min). The structure of albiflorin (**Figure 1**) included a benzoyl group, which might be hydrolysed by hydrolases present in the gut microbiota. Benzoic acid (**Figure 1**) was generated as a hydrolysate of albiflorin and was detected in the feces, plasma, and brain of mice (**Figure 2B**). The structure of benzoic acid was identified by high-resolution mass spectrometry and its nuclear magnetic resonance hydrogen spectrum (<sup>1</sup>H-NMR) and was ultimately confirmed by comparison with a reference substance. The <sup>1</sup>H-NMR data were as follows: <sup>1</sup>H

NMR (400 MHz, DMSO- $d_6$ ):  $\delta$ /ppm = 12.96 (s, 1 H, 9-H), 7.96 (d,  $J$  = 8.0 Hz, 2 H, 1-H, 5-H), 7.63 (t,  $J$  = 7.2 Hz, 1 H, 3-H), 7.51 (m, 2 H, 2-H, 4-H).

Besides benzoic acid, two other possible metabolites were formed in the gut bacteria. Alb-M2, eluted at 58.94 min, had an  $[M+H]^+$  at  $m/z$  299.2635 and an  $[M-H]^-$  at  $m/z$  297.2422, so the molecular weight of Alb-M2 was 298 (Figure S1-S2). Compared with the molecular weight of albiflorin, 182 Da was

lost from the parent drug. Alb-M2 did not have ultraviolet absorption. It was speculated that Alb-M2 was formed by albiflorin losing one each of BA,  $CO_2$ , and  $H_2O$  under the action of gut microbiota (Figure S1). Alb-M1, eluted at 35.71 min, had an  $[M+H]^+$  at  $m/z$  327.1028, which was 28 Da more than that of Alb-M (Figure S1-S2). Alb-M1 was possibly formed by Alb losing a BA and two  $H_2O$  (Figure S1).

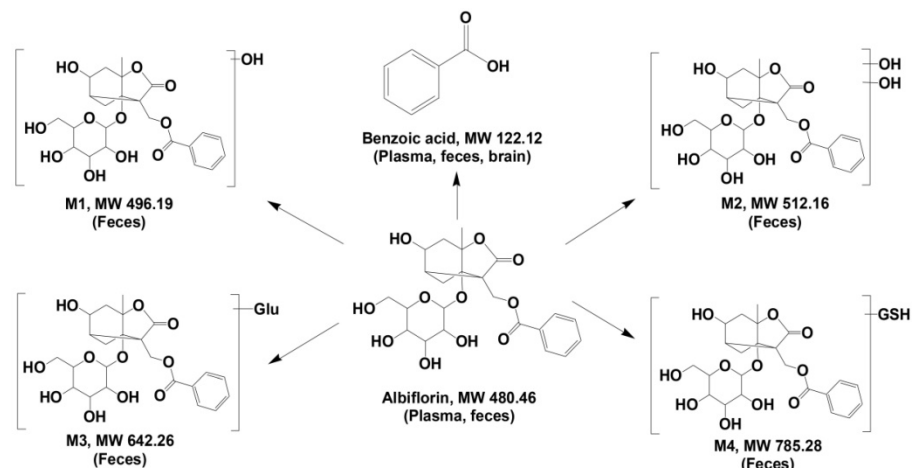


**Figure 1. Identification of albiflorin metabolites.** Five metabolites of albiflorin (Alb) were identified in mice. M1, M2, M3, and M4 were only detected in the feces of mice. Benzoic acid (BA) was detected in plasma, feces and brain.

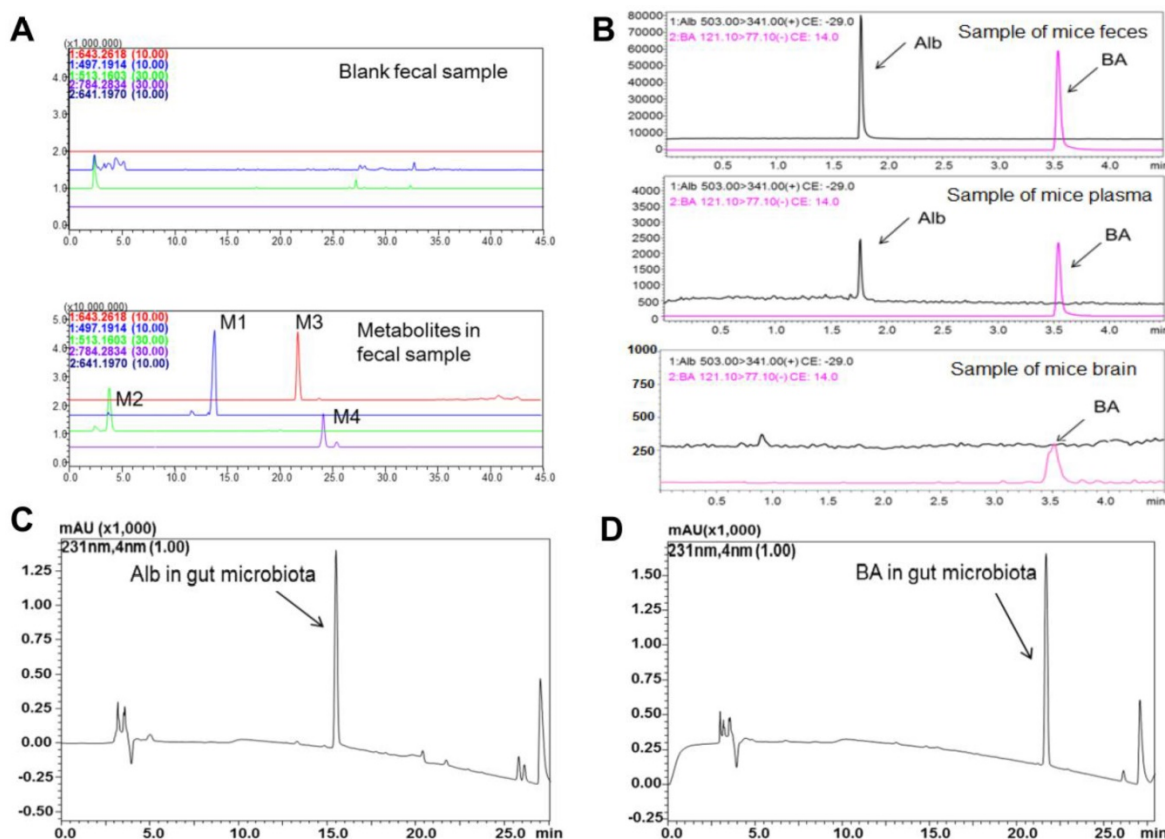


**Figure 2. Albiflorin metabolized by the gut microbiota *in vitro*.** (A) TIC of the metabolites in the blank and the fecal samples after treatment with albiflorin. (B) Albiflorin (Alb) and benzoic acid (BA) in the feces, plasma, and brain samples of the mice detected by LC-MS/MS. (C-D) Determination of albiflorin and benzoic acid in gut microbiota *in vitro* after incubation for 12 h.

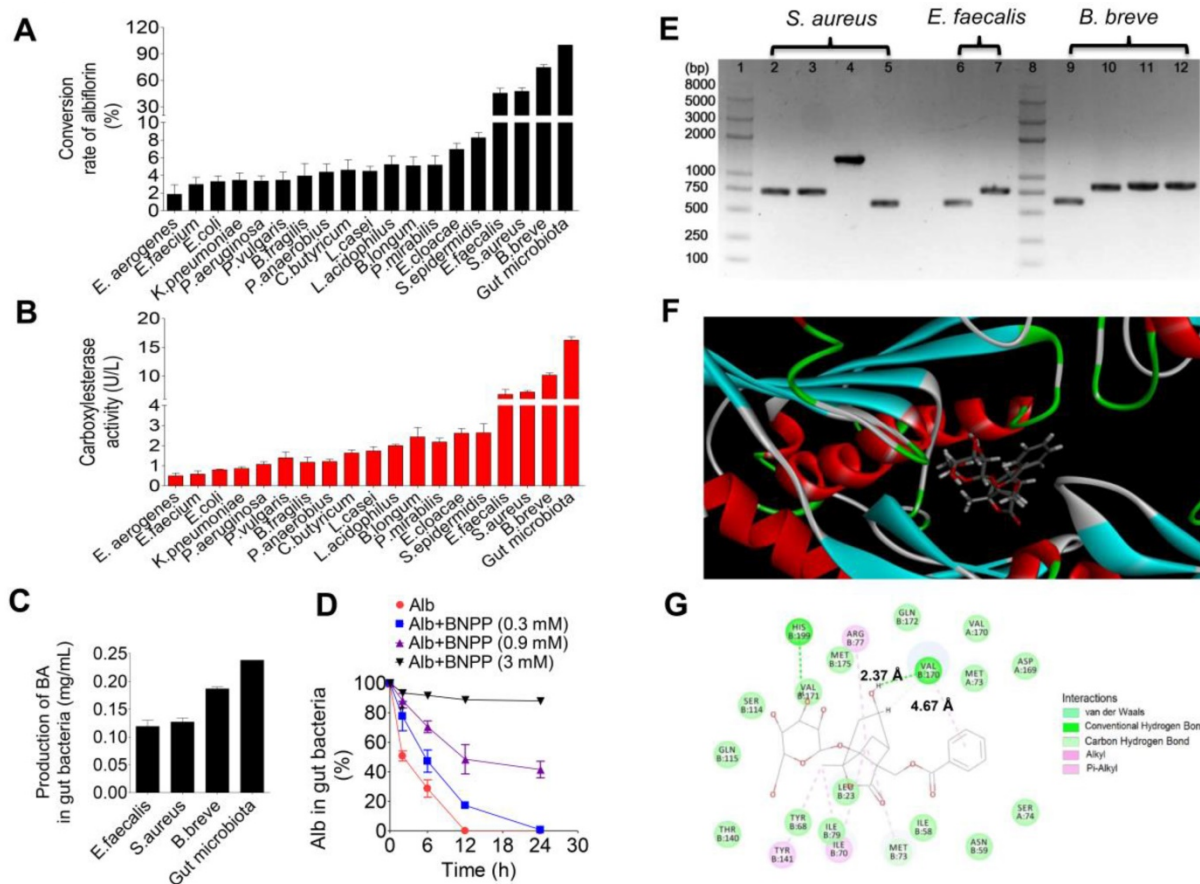


**Figure 3. Conversion of albiflorin to benzoic acid by carboxylesterase in gut microbiota. (A)** Conversion rate of albiflorin in the 18 strains and the gut microbiota. Three strains had strong conversion ability, *E. faecalis* (45.35%), *S. aureus* (47.55%) and *B. breve* (74.55%). **(B)** Enzyme activity assay of carboxylesterase in the 18 strains and the gut microbiota. Strains with the strongest enzyme activity were *E. faecalis*, *S. aureus* and *B. breve*, which were consistent with the results of albiflorin metabolism. **(C)** Benzoic acid (BA) generated by gut microbiota. The concentrations were 0.12 mg/mL by *E. faecalis*, 0.13 mg/mL by *S. aureus*, 0.19 mg/mL by *B. breve*, and 0.24 mg/mL by rat gut microbiota (as the positive control). **(D)** Carboxylesterase-mediated albiflorin (Alb) hydrolysis. The albiflorin conversion was inhibited by bis-p-nitrophenyl phosphate (BNPP, 0.3, 0.9 and 3 mM) with conversion rates of 100%, 82.7%, 51.5% and 11.3%. **(E)** Agarose gel electrophoresis of carboxylesterase genes PCR amplified from *E. faecalis*, *S. aureus*, and *B. breve*. 1, 8: Trans 2K plus II DNA marker; 2-5: carboxylesterase genes from *S. aureus*; 6 and 7: carboxylesterase genes from *E. faecalis*; 9-12: carboxylesterase genes from *B. breve*. **(F-G)** Molecular docking between albiflorin and carboxylesterase showed the chemical mechanism of albiflorin hydrolysis by carboxylesterase.

### Conversion of albiflorin to benzoic acid by carboxylesterase in gut microbiota

Eighteen standard strains of bacteria present in the gut microbiota were individually used to investigate albiflorin metabolism under anaerobic conditions for 12 h. As shown in **Figure 3A**, all 18 standard bacterial strains could convert albiflorin to benzoic acid with efficiencies ranging from 1.68% to 74.55% when the SD rat gut microbiota was set to 100% as the positive control. Three strains had a strong ability to convert albiflorin and resulted in a high value of conversion rate, including *E. faecalis* at 45.35%, *S. aureus* at 47.55% and *B. breve* at 74.55%. Accordingly, benzoic acid was generated in the incubation system with different concentrations at 0.12, 0.13 or 0.19 mg/mL by *E. faecalis*, *S. aureus*, and *B. breve*, respectively, compared to the positive control by the gut microbiota at 0.24 mg/mL (**Figure 3C**).

Next, the enzymatic activity of carboxylesterase

was measured to confirm whether the enzyme catalyzed the hydrolysis of albiflorin to benzoic acid. As shown in **Figure 3B**, the enzymatic activity of carboxylesterase in the 18 standard strains was sorted by albiflorin conversion ability. A positive correlation between the activity of this enzyme and formation of benzoic acid was observed. Strains with the strongest enzyme activity were *E. faecalis*, *S. aureus* and *B. breve*, consistent with the amount of benzoic acid production.

Addition of the carboxylesterase inhibitor bis-p-nitrophenyl phosphate (BNPP, 0.3, 0.9 and 3 mM) to the incubation system significantly inhibited the conversion of albiflorin to benzoic acid with inhibition rate in the range of 17.3%-88.74% at 12 h (**Figure 3D**), suggesting that the carboxylesterase of the gut microbiota might be an important bacterial enzyme that converts albiflorin into benzoic acid. We searched the amino acid sequence of carboxylesterase in the NCBI database using bioinformatic analysis.



There were two amino acid sequences in *E. faecalis* (WP\_002361880.1 and WP\_002362569.1), four amino acid sequences in *S. aureus* (WP\_001220807.1, WP\_001165962.1, WP\_000700912.1 and WP\_000400032.1), and four amino acid sequences in *B. breve* (WP\_003829800.1, WP\_003829196.1, WP\_003828396.1, and WP\_003828023.1). After transforming amino acid sequences into nucleotide sequences, carboxylesterase genes of *E. faecalis*, *S. aureus*, and *B. breve* were amplified by PCR. Agarose gel electrophoresis analysis showed that *S. aureus*, *E. faecalis*, and *B. breve* all contained carboxylesterase genes (**Figure 3E**). There were four genes of carboxylesterase (2-5 in **Figure 3E**) in *S. aureus*, including two sequences of 750 bp, one sequence of 500 bp and one sequence of 1500 bp. Two genes of carboxylesterase were found (6-7, in **Figure 3E**) in *E. faecalis* including one sequence of 750 bp and another of 500 bp. There were four carboxylesterase genes in *B. breve* (9-12, in **Figure 3E**) including three sequences of 750 bp and one of 500.

Carboxylesterase is a hydrolase that is present in a wide range of animal cells and gut microbiota. Since the crystal structure of carboxylesterase has been solved and is available in the PDB [38, 39], we performed a computer-assisted docking analysis of the initial binding step. The putative chemical mechanism for the docking of albiflorin with carboxylesterase is shown in **Figure 3F**. The two structures exhibited excellent docking performance when albiflorin docked onto carboxylesterase with a binding free energy of  $-21.15$  kcal/mol. The analysis of the binding mode of albiflorin with the enzyme revealed interactions with the conserved active site residues of carboxylesterase. As shown in **Figure 3G**, the presence of hydrophilic contacts (hydrogen bond) with a considerable number of residues in the active site appeared to be pivotal for albiflorin binding. Simultaneously, the presence of hydrophobic contacts (conjugation effect) also contributed to binding. For example, valine 170 interacted with two hydroxyl groups of the albiflorin molecule via two hydrogen bonds with an interaction distance of  $2.37$  Å. Moreover, hydrophobic interaction occurred between the valine and benzene ring of the albiflorin molecule with an interaction distance of  $4.67$  Å.

### Carboxylesterase-mediated conversion of albiflorin to benzoic acid

The activity of carboxylesterase was detected in the liver and the gut microbiota of normal mice as well as in the liver of mice treated with antibiotics. As shown in **Figure 4A**, the activity of carboxylesterase was unchanged in the liver of the mice treated with antibiotics compared to the normal mice (*NS*, no

significance). But, the activity of carboxylesterase in the gut microbiota was 9.1-fold higher than that in the liver ( $***P < 0.001$ ). Accordingly, benzoic acid generation in the gut microbiota was 44% higher than that in the liver after 1 h of incubation at  $37$  °C (**Figure 4B**).

### Benzoic acid might inhibit DAAO in the brain to exert its antidepressant effect

Benzoic acid, as an inhibitor of D-amino acid oxidase (DAAO), has been reported to prevent the degradation of D-amino acids particularly of D-serine [40-42]. Hence, D-serine (as a substrate probe) as well as the positive DAAO inhibitor AS057278 (as the control) was used to verify the effect of benzoic acid in the DAAO oxidation reaction system *in vitro* (**Figure 4C**). The results showed benzoic acid had a similar capacity to inhibit DAAO as the positive inhibitor AS057278 and resulted in increased D-serine with a production rate of 32% at the benzoic acid concentration of  $89$  μM (*vs* the normal group,  $***P < 0.001$ ). When AS057278 was used, D-serine had 38% serine production in the DAAO incubation assay (*vs* the normal group,  $***P < 0.001$ ), suggesting benzoic acid is a potential inhibitor of DAAO. Compared to benzoic acid, the parent drug albiflorin had no effect on DAAO in the brain homogenate *in vitro* (**Figure 4C**). The activity of DAAO was also determined in the brain after treatment with benzoic acid or albiflorin (**Figure 4D**). The result showed that benzoic acid (5 and  $10$  μg/mL) could significantly inhibit the activity of DAAO with a dose-dependent trend ( $***P < 0.001$ ); however, albiflorin had no effect on the activity of DAAO. These results further showed that benzoic acid might inhibit DAAO in the brain and exert an antidepressant effect.

### Pharmacokinetic study of albiflorin *in vivo*

The plasma concentration-time profiles of albiflorin were determined after three single *p.o.* doses of 3.5, 7, or  $14$  mg/kg and a single *i.v.* dose of  $1.75$  mg/kg (**Figure 5A-B**). The AUCs ( $_{0-\infty}$ ) of three single *p.o.* doses were  $2341.8 - 4263.0$  ng/mL min, which had a linear increase depending on the oral dose. The absolute oral bioavailability was determined to be 5.4% using the formula:  $F = AUC_{po} \times D_{iv} / AUC_{iv} \times D_{po} \times 100\%$ , based on the AUC ( $_{0-\infty}$ ) values calculated from *i.v.* and *p.o.* administration.

Because of the blood-brain barrier (BBB), albiflorin was not detected in the brain 2 h after ICR mice were orally administered albiflorin ( $14$  mg/kg) (**Figure 5C**). Instead of albiflorin, the characteristic metabolite of gut microbiota, benzoic acid, was detected in the brain after oral administration of albiflorin. Pseudo-germ-free (PGF) mice were used to



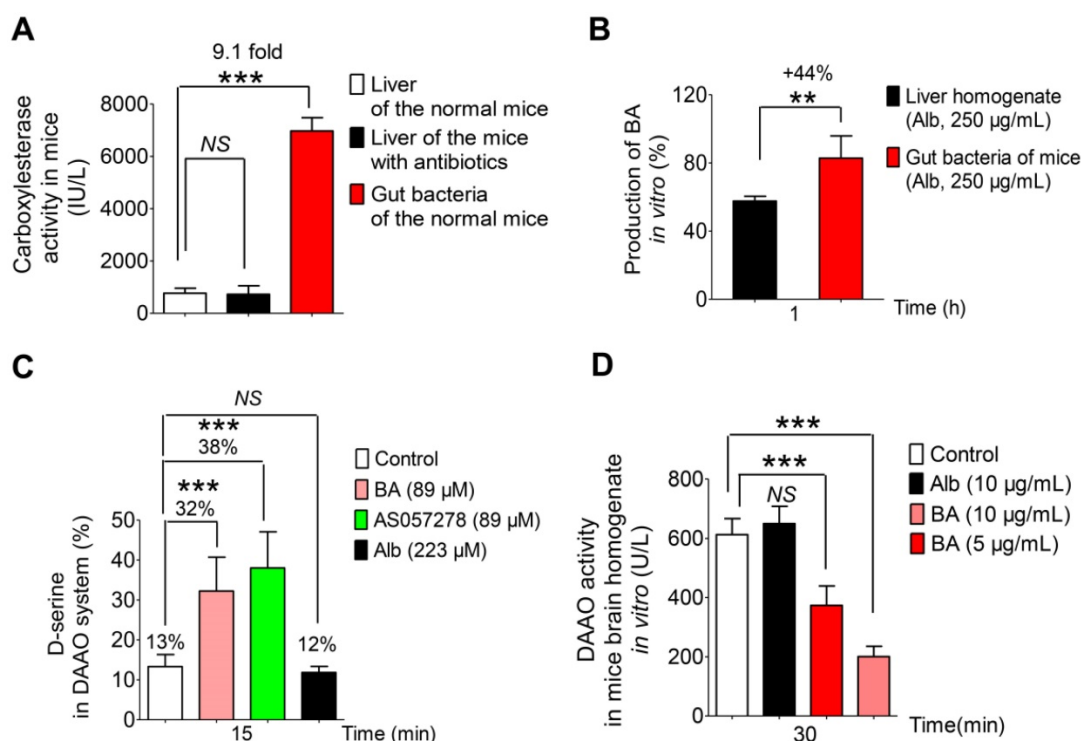


**Figure 4. Benzoic acid produced by the gut microbiota inhibited D-amino acid oxidase in the brain.** (A) The activity of carboxylesterase in the liver and gut microbiota of normal mice and in the liver of antibiotic-treated mice. (B) The percentage of the generated benzoic acid (BA) in the liver homogenate and the gut microbiota of mice after incubation with albiflorin (Alb, 250 µg/mL) at 37 °C for 1 h. (C) The percentage of the remaining D-serine in pure D-amino acid oxidase (DAAS) system *in vitro*. (D) The activity of D-amino acid oxidase in mice brain homogenate after treatment with benzoic acid (5 µg/mL, 10 µg/mL) and albiflorin (10 µg/mL). NS: no significance.

evaluate the pharmacokinetics of albiflorin and benzoic acid. The number of colony-forming units (CFU) is shown in Figure 5D. Mice treated with antibiotics displayed significantly fewer CFUs than the control group ( $***P < 0.001$ ) with an inhibitory rate of 71%.

Next, after the normal and the PGF mice were orally administered albiflorin (14 mg/kg), the drug concentration-time curves of albiflorin and benzoic acid were plotted (Figure 5E-G). In Figure 5G, the  $T_{max}$  value of benzoic acid (45 min) was slightly delayed compared with that of albiflorin (30 min). The  $C_{max}$  values of albiflorin and benzoic acid were at 86.2 and 55.5 ng/mL, respectively. Both albiflorin and benzoic acid were absorbed and eliminated rapidly. The amount of benzoic acid in the blood of PGF mice was much less than that in the blood of normal mice (Figure 5F). The  $C_{max}$  and  $AUC_{(0-t)}$  of benzoic acid in the normal mice blood were 1.73-fold and 1.74-fold higher than those of PGF mice. It is of note that albiflorin was not detected in mice brain despite the presence of benzoic acid (Figure 5C). After the oral administration of albiflorin, the concentration of benzoic acid in the brain was similar to that in the blood, with a  $T_{max}$  of 2 h and a  $C_{max}$  of 42.7 ng/mL. Benzoic acid in the PGF mice brain was much less than that in the normal mice brain (Figure 5E). The

$C_{max}$  and  $AUC_{(0-t)}$  of benzoic acid in the normal mice brain were 2.1-fold and 2.2-fold higher than those in the brains of PGF mice. These pharmacokinetic results suggested that the gut microbiota might regulate the conversion of albiflorin to benzoic acid in the intestine, which could then enter the blood and cross the blood-brain barrier in mice.

### Antidepressant activity of albiflorin in animals

To establish a depression model, SD rats were exposed to multiple alternating stimuli for 8 weeks. The sugar preference test was used to evaluate the degree of depressive symptoms in rats. The results of the sugar preference tests are shown in Figure 6A. Sugar preference values were 73.78% and 45.82% in the normal group and depression group, respectively, with a significant difference ( $***P < 0.001$ ). Thus, the chronic stress-induced depression model was successfully established for the subsequent treatment of albiflorin. After 14 days of treatment of depression model rats with albiflorin, the therapeutic outcome was plotted (Figure 6B). The sugar preference values of the depression group were significantly lower than those of the normal group ( $**P < 0.01$ ). The values of the two albiflorin groups (7 mg/kg and 14 mg/kg, orally) were both significantly higher than those of the depression group ( $*P < 0.05$ ,  $**P < 0.01$ ), showing a

dose-dependent response. The values of the benzoic acid group (14 mg/kg, orally) were significantly higher than those of the depression group (\*\* $P < 0.01$ ) and reached the normal level, suggesting that benzoic acid had an antidepressant activity similar to that of the albiflorin group (14 mg/kg). Compared with the values in the albiflorin (14 mg/kg) group, the sugar preference values in the PGF group decreased significantly (\*\* $P < 0.01$ ), indicating that the gut microbiota might mediate the therapeutic efficacy of albiflorin. The concentration of benzoic acid in the brain was determined by LC-MS/MS to investigate the relationship between benzoic acid and the therapeutic efficacy of albiflorin (Figure 6C). The benzoic acid concentration in the brain of the albiflorin groups (7 mg/kg and 14 mg/kg) increased in a dose-dependent manner, and the concentration in the 14 mg/kg group was 1.6-fold higher than that in the 7 mg/kg group. The benzoic acid concentration was also measured in PGF rats ( $17.16 \pm 6.21$  ng/mL) and was significantly lower than that in the normal

mice treated with 14 mg/kg albiflorin ( $37.26 \pm 15.70$  ng/mL, \*\* $P < 0.01$ ). The therapeutic efficacy of albiflorin was proportional to the benzoic acid concentration in the rat brain. Based on these findings, it is plausible that conversion of albiflorin to benzoic acid by the gut microbiota might be the molecular mechanism of the antidepressant activity of albiflorin after oral administration. The forced swimming test was also performed using ICR mice to evaluate the antidepressant activity of albiflorin. Two hours after the albiflorin treatment, ICR mice were forced to swim for 5 min. Immobility time in the last 3 min was recorded (Figure 6D). The groups orally administered 7 mg/kg and 14 mg/kg albiflorin spent 11.4% and 20.5% less time immobile, respectively, than the control group ( $*P < 0.05$ ). The PGF mice treated with 14 mg/kg orally administered albiflorin spent 18.6% more time immobile than the albiflorin group, indicating that the gut microbiota might mediate the antidepressant activity of albiflorin.

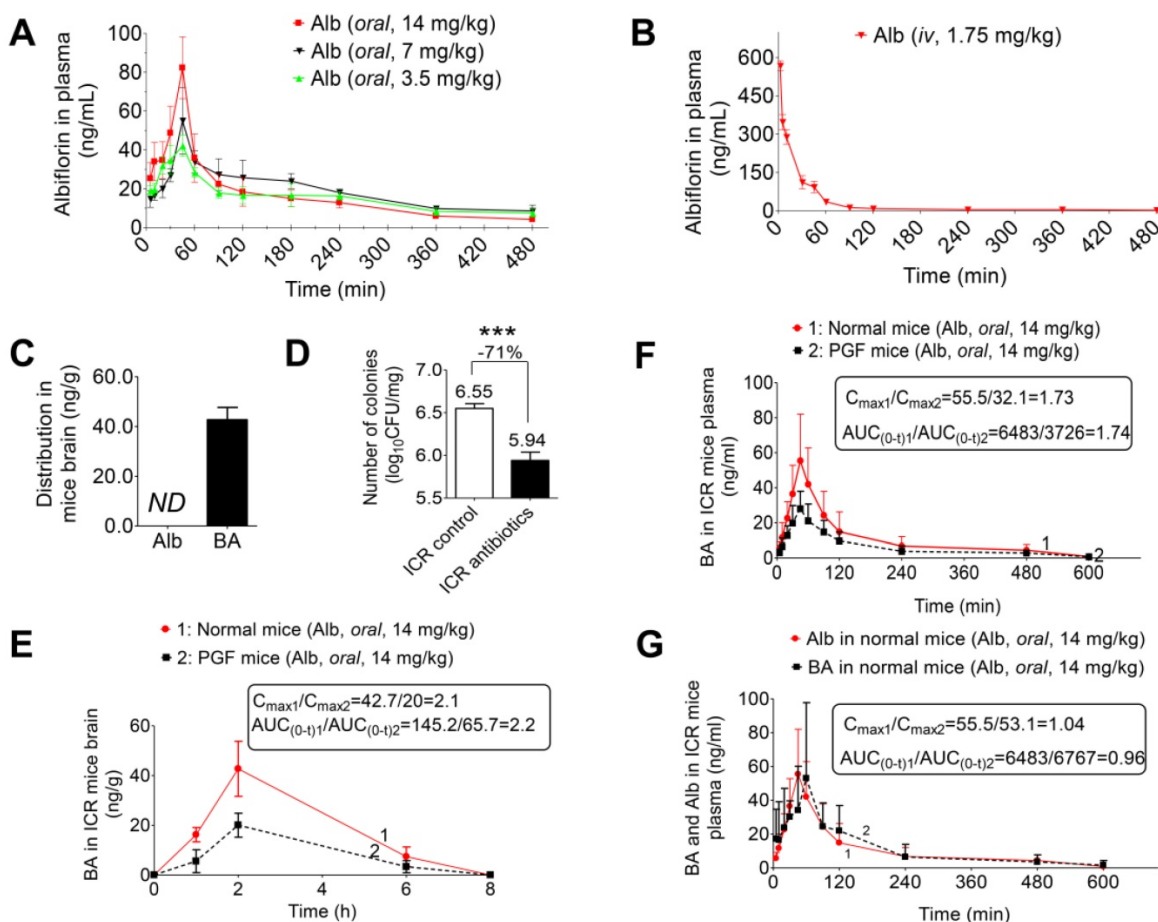


**Figure 5. Pharmacokinetic study of albiflorin in vivo.** (A) Plasma concentration-time profiles of albiflorin (Alb) in mice after oral administration (3.5, 7, and 14 mg/kg). (B) Plasma concentration-time profiles of albiflorin in mice after intravenous injection of albiflorin (1.75 mg/kg). (C) Brain distribution of albiflorin and benzoic acid (BA) in mice 2 h after oral treatment with albiflorin (14 mg/kg). ND: not detected. (D) Number of colonies from normal and PGF mice. Colonies were significantly inhibited (71%) by antibiotics (\*\* $P < 0.001$ ). (E) Benzoic acid concentrations in the brains of normal and pseudo-germ-free (PGF) mice after oral administration of albiflorin (14 mg/kg). The  $C_{max}$  and  $AUC_{(0-1)}$  of the normal mice were 2.1- and 2.2-fold higher than those of PGF mice, respectively. (F) Benzoic acid in the plasma of normal and PGF mice after oral administration of albiflorin (14 mg/kg). The  $C_{max}$  and  $AUC_{(0-1)}$  of the normal mice were 1.73- and 1.74- fold higher than those of PGF mice. (G) Blood concentrations of benzoic acid and albiflorin in normal ICR mice after treatment with albiflorin (14 mg/kg).

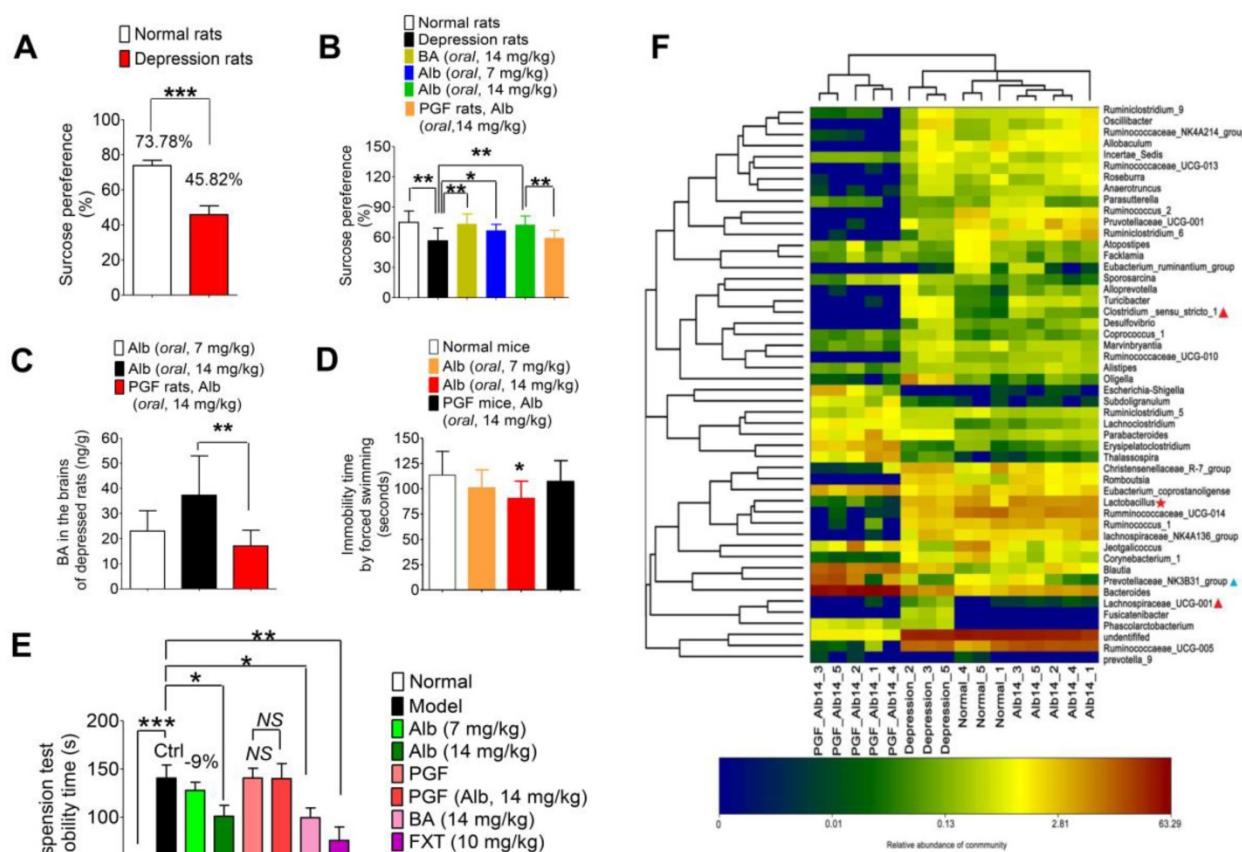


**Figure 6. Antidepressant activity of albiflorin.** (A) Sugar preference tests after 8 weeks of stimulation. Sugar preference values of the model group were significantly lower than those of the normal group (\*\* $P < 0.01$ ). (B) Sugar preference tests after 2 weeks of treatment with albiflorin (Alb) or benzoic acid (BA). Sugar preference values of the benzoic acid group (14 mg/kg) and the albiflorin groups (7 and 14 mg/kg) were significantly higher than those in the model group. Sugar preference values of the pseudo-germ-free (PGF) group were significantly lower than those in the albiflorin group (14 mg/kg) (\*\* $P < 0.05$ , \*\*\* $P < 0.001$ ). (C) Benzoic acid concentration in the brains of depressed rats. Benzoic acid concentrations in the brains of rats in the albiflorin groups (7 and 14 mg/kg) increased in a dose-dependent manner. The benzoic acid concentration in PGF rats was significantly lower than that in the albiflorin group (oral, 14 mg/kg, \*\* $P < 0.01$ ). (D) Immobility time during the forced swimming test using ICR mice. The immobility time of the albiflorin groups (7 and 14 mg/kg) decreased in a dose-dependent manner. The immobility time of the albiflorin (14 mg/kg) group was significantly less than that of the control group (\* $P < 0.05$ ). (E) Immobility time of the tail suspension test in the reserpine-induced mouse acute depression model. The immobility time of the albiflorin group (14 mg/kg) and benzoic acid group (14 mg/kg) decreased significantly (\* $P < 0.05$ ) compared with the model group; the immobility time of the positive control group (fluoxetine, FXT, 10 mg/kg) showed a significant effect (\*\* $P < 0.01$ ). The immobility time remained unchanged in the PGF group when treated with albiflorin (14 mg/kg). (F) Bacterial composition modified by albiflorin. The heat-map shows the top 50 bacterial genera with the most substantial change in abundance after establishment of the depression model and treatment with albiflorin. The color of the spot corresponds to the normalized and log-transformed relative abundance of genera. The change of color from blue to red represents corresponding colony abundance. ☆ (red) Depression-related bacteria with abundance increased after treatment with albiflorin. ▲ (blue) Depression-related bacteria with abundance increased (red) and decreased (blue) after stimulation.

Additionally, a reserpine-induced acute depression model was established to verify the antidepressant effect of albiflorin using fluoxetine as the positive control (Figure 6E). The tail suspension test was carried out 1.5 h after reserpine injection (*i.p.*, 4 mg/kg) and the immobility time was recorded as shown in Figure 6E. The acute model was successfully established with significantly longer immobility time (normal group *vs* model group:  $50.0 \pm 7.6$  s *vs*  $140.6 \pm 13.6$  s, \*\*\* $P < 0.001$ ). After treatment with 14 mg/kg albiflorin or benzoic acid for 7 days, the values of immobility time in the tail suspension test showed an obvious decrease of  $101.1 \pm 11.2$  s (\* $P < 0.05$ ) and  $99.5 \pm 10.1$  s (\* $P < 0.05$ ), respectively, compared with  $140.6 \pm 13.6$  s in the model group. The fluoxetine group

showed a better effect with an immobility time of  $76.0 \pm 17.8$  s (\*\* $P < 0.01$ ). As for the two PGF groups, the immobility time was almost the same with or without albiflorin treatment with values of  $140.6 \pm 10.1$  s in the PGF group and  $140.0 \pm 15.6$  s in the albiflorin-treated PGF group.

Furthermore, three other typical indicators including body temperature, the degree of ptosis, and the out-circle rate were recorded after reserpine injection (Table 2). The body temperature in the model group ( $34.55 \pm 0.25$  °C) was significantly lower than that of the normal group ( $37.10 \pm 0.60$  °C, \*\*\* $P < 0.001$ ). The efficacy was obvious by the body temperatures in the high-dose albiflorin group (14 mg/kg,  $35.21 \pm 0.51$  °C), the benzoic acid group (14



mg/kg,  $35.23 \pm 0.40$  °C), and the fluoxetine positive control group (10 mg/kg,  $35.31 \pm 0.26$  °C) (\*\* $P < 0.01$ , \*\*\* $P < 0.001$ , \*\*\* $P < 0.001$ ). Similar results were observed in the ptosis score and out-circle rate. The mean score of ptosis was decreased to a value of 1.8 in the albiflorin group (14 mg/kg, \* $P < 0.05$ ), 1.7 in the benzoic acid group (14 mg/kg, \* $P < 0.05$ ), and 1.4 in the fluoxetine group (10 mg/kg, \* $P < 0.05$ ) compared with the model group with the mean value 2.7. The results also showed positive effects in the out-circle rate test with 70% for the albiflorin group (14 mg/kg, \* $P < 0.05$ ), 70% for the benzoic acid group (14 mg/kg, \* $P < 0.05$ ) and 60% for the fluoxetine group (10 mg/kg) vs 20% for the model group (NS: no significance). The effect of albiflorin (14 mg/kg) in the PGF group was weak and not significant. The combined results clearly indicated the important role of gut microbiota in mediating the antidepressant activity of albiflorin in animals, which appeared to be similar to that of the positive control fluoxetine.

**Table 2.** The results of body temperature and behavior performance in reserpine-induced acute depression models.

Group	Dose (mg/kg)	Body temperature <sup>1</sup> (°C)	Mean score of ptosis <sup>2</sup>	Rate of out-circle <sup>3</sup> (%)
Normal	-	37.10±0.60	0	100.0
Model (Ctrl)	-	34.55±0.25 #,***	2.7 #,***	20.0 #,***
Alb-L	7	34.74±0.50	2.1	40.0
Alb-H	14	35.21±0.51 **	1.8 *	70.0 *
PGF	-	34.16±0.50	2.8	30.0
PGF+Alb	14	34.49±0.58	2.7	20.0
BA	14	35.23±0.40 ***	1.7 *	70.0 *
FXT	10	35.31±0.26 ***	1.4 *	60.0

Normal: normal control group; Model: reserpine-induced group; Alb-L: low-dose albiflorin group; Alb-H: high-dose albiflorin group; PGF: combined antibiotics-treated pseudo-germ-free group; PGF+Alb: PGF treated with albiflorin group; BA: benzoic acid group; FXT: fluoxetine group.

# Model group vs normal group, \*\* $P < 0.01$ , \*\*\* $P < 0.001$ .

<sup>1</sup> Mean body temperatures expressed as mean ± SD, \*\* $P < 0.01$ , \*\*\* $P < 0.001$ .

<sup>2</sup> Mean score of ptosis, \* $P < 0.05$ .

<sup>3</sup> Rate of out-circle (%), \* $P < 0.05$ .

All data were analyzed by double-tailed t-test compared with the model group.

## Bacterial composition modified by albiflorin

The gut microbiota composition was analyzed by sequencing the 16S rRNA gene. SD rats were orally administered albiflorin or albiflorin plus antibiotics for 14 days, and fecal samples were collected for bacterial composition analysis. The barcoded pyrosequencing of the V3 and V4 regions of the 16S rRNA gene showed that the gut microbiota of depressed rats was dysregulated and albiflorin had the ability to regulate the gut microbiota composition. A heat map of the top 50 bacterial genera that exhibited the most substantial changes in abundance after exposure to albiflorin is displayed in **Figure 6F**. Out of the 50 genera, the abundance of 14 genera (*Sporosarcina*, *Alloprevotella*, *Turicibacter*, *Clostridium*,

*Desulfovibrio*, *Coprococcus*, *Marvinbryantia*, *Ruminococcaceae*, *Oligella*, *Parabacteroides*, *Blautia*, *Lachnospiraceae*, *Fusicatenibacter*, and *Phascolarctobacterium*) increased and the abundance of 7 genera (*Prevotellaceae*, *Jeotgalicoccus*, *Ruminococcaceae*, *Facklamia*, *Atopostipes*, *Ruminiclostridium*, *Ruminococcus*) decreased in the gut microbiota of depressed rats compared with their abundance in normal rats. *Lachnospiraceae*, *Clostridium*, and *Prevotellaceae* were reported to be related to depression; *Lachnospiraceae* levels increased in social defeat-stressed mice [43], and *Clostridium difficile* infection was related to depression [44].

After 14 days of albiflorin treatment, the composition of the gut microbiota of depressed rats improved to a certain extent; the abundance of 4 genera, *Prevotellaceae*, *Lactobacillus*, *Ruminococcaceae* and *Ruminococcus*, increased with a simultaneous decrease in the abundance of 7 genera, *Phascolarctobacterium*, *Fusicatenibacter*, *Lachnospiraceae*, *Parabacteroides*, *Oligella*, *Sporosarcina* and *Turicibacter*. The transfer of *Ruminococcaceae* to nonobese diabetic mice modulated their social behavior [45]; and *Lactobacillus*, a known probiotic, was thought to improve symptoms of depression and anxiety [46]. The abundance of these two genera increased after albiflorin treatment, suggesting that albiflorin might be able to regulate the composition of the gut microbiota in depressed rats by increasing the abundance of the potential probiotics. *Parabacteroides goldsteinii* was isolated from the blood culture of a patient with complications of intra-abdominal infection [47], and *Oligella ureolytica* was found to be associated with bloodstream infections [48]. Also, *Turicibacter* was positively correlated with acute dextran sulfate sodium-induced colitis [49]. As conditional pathogenic bacteria, these strains were inhibited by albiflorin. In summary, albiflorin represents a likely treatment for depression that might modulate the potential probiotics and simultaneously inhibit conditional pathogenic bacteria in the gut microbiota.

## Discussion

As a natural product, albiflorin is present at low levels in the blood and brain after oral administration because of its poor bioavailability (5.4%) and its inability to cross the blood-brain barrier [50]. In our study, pharmacokinetic data showed that albiflorin could not be detected in the mouse brain by both LC-MS/MS and LC/MS<sup>n</sup>-IT-TOF, which indicated that it could not cross the blood-brain barrier after oral administration. The antidepressant mechanism of albiflorin has not been completely elucidated because of these obstacles.

As shown in the present study, the gut microbiota act as an “organ” that converts albiflorin to benzoic acid in the intestine via a hydrolysis reaction mediated by bacterial carboxylesterase. Benzoic acid, the inhibitor of D-amino acid oxidase (DAAO), prevents the degradation of D-amino acids, particularly of D-serine [40-42]. The evidence is most convincing for D-serine, which acts as a co-agonist for the N-methyl-D-aspartate receptor (NMDAR), a recognized receptor involved in learning, memory, and synaptic plasticity [51, 52]. Abnormal levels of D-amino acids have been reported in patients with depression and Alzheimer’s disease [53], suggesting a direct link between D-serine and depression. In a recent clinical trial, 52 patients with chronic schizophrenia were assigned to placebo or adjunct sodium benzoate treatment for 6 weeks, which significantly improved a variety of symptoms and neurocognition [42]. A drug-naïve patient with major depressive disorder displayed a significant increase in subcortical volume after a 6-week therapy with sodium benzoate [54]. Based on the above evidence, benzoic acid appears to be effective against depression and other central nervous system diseases. In our study, benzoic acid exhibited a significant antidepressant effect. The antidepressant efficacy of albiflorin appeared to be due to its specific metabolite, benzoic acid, which was produced by the gut microbiota.

We used 18 standard strains of bacteria from the gut microbiota to determine whether benzoic acid was a characteristic metabolite of albiflorin generated by the gut microbiota and to verify that albiflorin hydrolysis was proportional to the generation of benzoic acid. Based on the results of molecular docking, treatments with specific inhibitors, as well as gene comparison analysis, carboxylesterase might be one of the key metabolic enzymes converting albiflorin to benzoic acid. By pharmacokinetic analysis of albiflorin and benzoic acid in animals, we verified that albiflorin did not pass through the blood-brain barrier. In contrast, benzoic acid readily crossed the blood-brain barrier as its level in the brain increased after the oral administration of albiflorin. Moreover, the brain benzoic acid levels were significantly reduced in mice treated with antibiotics compared with normal mice after the oral administration of albiflorin. Because the antibiotics inhibited the gut microbiota, production of benzoic acid was decreased and its concentrations in the blood and brain were reduced accordingly. Based on these observations, we concluded that benzoic acid was the specific metabolite of albiflorin derived from the gut microbiota, providing a possible molecular mechanism for the antidepressant effects of albiflorin.

We investigated the relationship between the antidepressant activity of albiflorin and gut microbiota, as well as the benzoic acid concentration in the brain. Albiflorin exhibited an excellent antidepressant activity in both the chronic stress-induced depression model and in the mouse forced swimming model. Albiflorin has recently been shown to play an important role in the treatment of depression [31], which validates the results of our study. Rats in the albiflorin group that were treated with antibiotics performed poorly in the sugar preference test, which was similar to the pharmacokinetics of benzoic acid *in vivo*. This observation suggested that the gut microbiota was associated with the therapy of albiflorin. A similar investigation related to gut bacteria was previously reported in which decreased efficacy of berberine was observed in *ob/ob* mice and KK-Ay mice after combined administration of antibiotics. As a natural medicine, berberine exerts blood lipid lowering effects mainly through the gut microbiota [55]. Therefore, we conjectured that the antidepressant activity of albiflorin was based on the gut microbiota and its therapeutic efficacy was proportional to the benzoic acid concentration in the rat brain. Benzoic acid, generated from albiflorin by the gut microbiota, was likely the molecular mechanism underlying the antidepressant activity of albiflorin. Furthermore, besides its conversion into benzoic acid, albiflorin also improved the composition of the gut microbiota of the depressed rats to achieve its antidepressant effect. The increase in probiotic bacteria (such as *Lactobacillus*) and decrease in pathogenic bacteria (such as *Parabacteroides*, *Oligella* and *Turicibacter*) may improve the health of the intestinal environment, potentially enabling it to be better able to resist diseases [37, 56-59].

In summary, we identified benzoic acid as a therapeutic mediator of albiflorin generated by the gut microbiota, substantiating the hypothesis of the gut-brain axis mechanism. Benzoic acid, after crossing the blood-brain barrier, entered the central nervous system to exert antidepressant effects. Benzoic acid was also beneficial for improving the bacteria composition, thus further enhancing the antidepressant effects. Our study has proposed a promising mechanism of the antidepressant therapy of albiflorin via the gut microbiota. The molecular details of the drug mechanism regulating the gut microbiota might open up new avenues in drug development for the treatment of depression.

## Abbreviations

Alb: albiflorin; BA: benzoic acid; BBB: blood-brain barrier; BNPP: bis-p-nitrophenyl

phosphate; CFU: colony-forming units; DAAO: D-amino acid oxidase; FXT: fluoxetine; LC/MS<sup>n</sup>-IT-TOF: liquid chromatography with ion trap time-of-flight mass spectrometer; LC-MS/MS: liquid chromatography with tandem mass spectrometry; MRM: multiple reaction monitoring; PGF: pseudo-germ-free.

## Supplementary Material

Supplementary figures and tables.

<http://www.thno.org/v08p5945s1.pdf>

## Acknowledgments

The project was supported by CAMS Innovation Fund for Medical Sciences (CIFMS) (No. 2016-I2M-3-011), the National Natural Science Foundation of China (No. 81573493), the Beijing Key Laboratory of Non-Clinical Drug Metabolism and PK/PD study (Z141102004414062) and the National Megaproject for Innovative Drugs (Nos. 2018ZX09711001-002-002 and 2018ZX09302015). We would like to thank Shimadzu (China) Co., Ltd for technological support.

## Author contributions

Y.W. and J.D.J. conceptualized the experiments and analyses. Z.X.Z., S.R.M. J.B.Y. and L.B.P. performed the animal experiments. R.P., S.R.M. and L.C. performed the molecular biology study. J.F. performed the biotransformation study. Z.G.Z. and H.T. provided the albiflorin compounds. C.T.C. identified the medicinal materials. Y.W. and Z.X.Z. wrote the paper.

## Competing Interests

The authors have declared that no competing interest exists.

## References

- Smith K. Mental health: a world of depression. *Nature*. 2014; 515: 181.
- Anthes E. Depression: a change of mind. *Nature*. 2014; 515: 185-7.
- Luscher B, Shen Q, Sahir N. The GABAergic deficit hypothesis of major depressive disorder. *Mol Psychiatry*. 2011; 16: 383-406.
- Guilloux JP, Douillard-Guilloux G, Kota R, Wang X, Gardier AM, Martinowich K, et al. Molecular evidence for BDNF- and GABA-related dysfunctions in the amygdala of female subjects with major depression. *Mol Psychiatry*. 2012; 17: 1130-42.
- Müller N, Schwarz MJ. The immune-mediated alteration of serotonin and glutamate: towards an integrated view of depression. *Int J Obes*. 2007; 12: 988-1000.
- Schlössera RGM, Wagnera G, Kocha K, Dahnke R, Reichenbachb JR. Fronto-cingulate effective connectivity in major depression: a study with fMRI and dynamic causal modeling. *Neuroimage*. 2008; 43: 645-55.
- Lu DY, Lu TR, Zhu PP, Che JY. The efficacies and toxicities of antidepressant drugs in clinics, building the relationship between Chemo-Genetics and Socio-Environments. *Cent Nerv Syst Agents Med Chem*. 2016; 16: 12-18.
- Whiskey E, Taylor D. A review of the adverse effects and safety of noradrenergic antidepressants. *J Psychopharmacol*. 2013; 27: 732-9.
- Voican CS, Corruble E, Naveau S, Perlemuter G. Antidepressant-induced liver injury: a review for clinicians. *Am J Psychiat*. 2014; 171: 404-15.
- O'Toole PW, Jeffery IB. Gut microbiota and aging. *Science*. 2015; 350: 1214-5.
- Bäumler AJ, Sperandio V. Interactions between the microbiota and pathogenic bacteria in the gut. *Nature*. 2016; 535: 85-93.

- Lozupone CA, Stombaugh JI, Gordon JI, Jansson JK, Knight R. Diversity, stability and resilience of the human gut microbiota. *Nature*. 2012; 489: 220-30.
- Honda K, Littman DR. The microbiota in adaptive immune homeostasis and disease. *Nature*. 2016; 535: 75-84.
- Chen J, Qiao Y, Tang B, Chen G, Liu X, Yang B, et al. Modulation of Salmonella tumor-colonization and intratumoral anti-angiogenesis by triptolide and its mechanism. *Theranostics*. 2017; 7: 2250-60.
- Kim JE, Phan TX, Nguyen VH, Dinh-Vu HV, Zheng JH, Yun M, et al. Salmonella typhimurium suppresses tumor growth via the pro-inflammatory cytokine interleukin-1 $\beta$ . *Theranostics*. 2015; 5: 1328-42.
- Donaldson GP. Indigenous bacteria from the gut microbiota regulate host serotonin biosynthesis. *Cell*. 2015; 161: 264-76.
- Foster JA, McVey Neufeld KA. Gut-brain axis: how the microbiome influences anxiety and depression. *Trends Neurosci*. 2013; 36: 305-12.
- Evrensel A, Ceylan ME. The gut-brain axis: the missing link in depression. *Clin Psychopharmacol Neurosci*. 2015; 13: 239-44.
- Schachter J, Martel J, Lin CS, Chang CJ, Wu TR, Lu CC, et al. Effects of obesity on depression: a role for inflammation and the gut microbiota. *Brain Behav Immun*. 2018; 69: 1-8.
- Winter G, Hart RA, Charlesworth RPG, Sharpley CF. Gut microbiome and depression: what we know and what we need to know. *Rev Neurosci*. 2018; 29: 629-43.
- Wang Y, Shou J, Jiang J. Metabolism of Chinese materia medica in gut microbiota and its biological effects. *Chin Herb Med*. 2015; 7: 109-15.
- Wang Y, Jiang J. A new research mode of drug PK-PD mediated by the gut microbiota: insights into the pharmacokinetics of berberine. *Acta Pharmaceutica Sinica (Chinese version)*. 2018; 53: 659-666.
- Kang DW, Adams JB, Gregory AC, Borody T, Chittick L, Fasano A, et al. Microbiota Transfer Therapy alters gut ecosystem and improves gastrointestinal and autism symptoms: an open-label study. *Microbiome*. 2017; 5: 10.
- Ma X, Zhao Y, Zhu Y, Chen Z, Wang J, Li R, et al. Paeonia lactiflora Pall. protects against ANIT-induced cholestasis by activating Nrf2 via PI3K/Akt signaling pathway. *Drug Des Devel Ther*. 2015; 9: 5061-74.
- Huang S, Wang R, Shi Y, Yang L, Wang Z, Wang Z. Primary safety evaluation of sulfated Paeoniae Radix Alba. *Acta Pharmaceutica Sinica (Chinese version)*. 2012; 47: 486-91.
- Xiaoxia Z, Linlin J, Chun C, Meng S, Qin F, Jianxin D, et al. Danzhi Xiaoyao San ameliorates depressive-like behavior by shifting toward serotonin via the downregulation of hippocampal indoleamine 2,3-dioxygenase. *J Ethnopharmacol*. 2015; 160: 86-93.
- Li Y, Sun Y, Ma X, Xue X, Zhang W, Wu Z, et al. Effects of Sini San used alone and in combination with fluoxetine on central and peripheral 5-HT levels in a rat model of depression. *J Tradit Chin Med*. 2013; 33: 674-81.
- Commission CP. Chinese Pharmacopoeia: Chinese Medical Science and Technology Press. 2015; I: 1354-1356.
- Wang YL, Wang JX, Hu XX, Chen L, Qiu ZK, Zhao N, et al. Antidepressant-like effects of albiflorin extracted from Radix paeoniae Alba. *J Ethnopharmacol*. 2016; 179: 9-15.
- Qiu ZK, He JL, Liu X, Zeng J, Chen JS, Hong N. Anti-PTSD-like effects of albiflorin extracted from Radix paeoniae Alba. *J Ethnopharmacol*. 2017; 198: 324-30.
- Song J, Hou X, Hu X, Lu C, Liu C, Wang J, et al. Not only serotonergic system, but also dopaminergic system involved in albiflorin against chronic unpredictable mild stress-induced depression-like behavior in rats. *Chem Biol Interact*. 2015; 242: 211-7.
- Jin ZL, Gao N, Xu W, Xu P, Li S, Zheng YY, et al. Receptor and transporter binding and activity profiles of albiflorin extracted from Radix paeoniae Alba. *Sci Rep*. 2016; 6: 33793.
- Fei F, Yang H, Peng Y, Wang P, Wang S, Zhao Y, et al. Sensitive analysis and pharmacokinetic study of the isomers paeoniflorin and albiflorin after oral administration of total glucosides of White Paeony Capsule in rats. *J Chromatogr B*. 2016; 1022: 30-7.
- He CY, Fu J, Shou JW, Zhao ZX, Ren L, Wang Y, et al. In vitro study of the metabolic characteristics of eight isoquinoline alkaloids from natural plants in rat gut microbiota. *Molecules*. 2017; 22: 932.
- Willner P. The validity of animal models of depression. *Psychopharmacology*. 1984; 83: 1-16.
- Finberg JP, Youdim MB. Pharmacological properties of the anti-Parkinson drug rasagiline; modification of endogenous brain amines, reserpine reversal, serotonergic and dopaminergic behaviours. *Neuropharmacology*. 2002; 43: 1110-8.
- Wang Y, Shou JW, Li XY, Zhao ZX, Fu J, He CY, et al. Berberine-induced bioactive metabolites of the gut microbiota improve energy metabolism. *Metabolism*. 2017; 70: 72-84.
- Chen Q, Luan ZJ, Cheng X, Xu JH. Molecular dynamics investigation of the substrate binding mechanism in carboxylesterase. *Biochemistry*. 2015; 54: 1841-8.
- Kim KK, Song HK, Shin DH, Hwang KY, Choe S, Yoo OJ, et al. Crystal structure of carboxylesterase from *Pseudomonas fluorescens*, an alpha/beta hydrolase with broad substrate specificity. *Structure*. 1997; 5: 1571-84.
- Lane HY, Lin CH, Green MF, Helleman G, Huang CC, Chen PW, et al. Add-on treatment of benzoate for schizophrenia: a randomized, double-blind, placebo-controlled trial of D-amino acid oxidase inhibitor. *JAMA Psychiatry*. 2013; 70: 1267-75.



41. Lin CH, Chen PK, Chang YC, Chuo LJ, Chen YS, Tsai GE, et al. Benzoate, a D-amino acid oxidase inhibitor, for the treatment of early-phase Alzheimer disease: a randomized, double-blind, placebo-controlled trial. *Biol Psychiatry*. 2014; 75: 678-85.
42. Tsai GE. Impact of dietary benzoic acid on treatment response in schizophrenia—reply. *JAMA Psychiatry*. 2014; 71: 1298-9.
43. Aokiyoshida A, Aoki R, Moriya N, Goto T, Kubota Y, Toyoda A, et al. Omics studies of the murine intestinal ecosystem exposed to subchronic and mild social defeat stress. *J Proteome Res*. 2016; 15: 3126-38.
44. Rogers MA, Greene MT, Young VB, Saint S, Langa KM, Kao JY, et al. Depression, antidepressant medications, and risk of *Clostridium difficile* infection. *BMC Med*. 2013; 11: 121.
45. Gacias M, Gaspari S, Santos PM, Tamburini S, Andrade M, Zhang F, et al. Microbiota-driven transcriptional changes in prefrontal cortex override genetic differences in social behavior. *eLife*. 2016; 5: e13442.
46. Naseribafrouei A, Hestad K, Avershina E, Sekelja M, Linlökken A, Wilson R, et al. Correlation between the human fecal microbiota and depression. *Neurogastroenterol Motil*. 2014; 26: 1155-62.
47. Awadelkariem FM, Patel P, Kapoor J, Brazier JS, Goldstein EJC. First report of *Parabacteroides goldsteinii* bacteraemia in a patient with complicated intra-abdominal infection. *Anaerobe*. 2010; 16: 223-5.
48. Demir T, Celenk N. Bloodstream infection with *Oligella ureolytica* in a newborn infant: a case report and review of the literature. *J Infect Dev Ctries*. 2014; 8: 793-5.
49. Munyaka PM, Rabbi MF, Khafipour E, Ghia JE. Acute dextran sulfate sodium (DSS)-induced colitis promotes gut microbial dysbiosis in mice. *J Basic Microbiol*. 2016; 56: 986-98.
50. Huang X, Su S, Cui W, Liu P, Duan JA, Guo J, et al. Simultaneous determination of paeoniflorin, albiflorin, ferulic acid, tetrahydropalmatine, protopine, typhaneoside, senkyunolide I in beagle dogs plasma by UPLC-MS/MS and its application to a pharmacokinetic study after oral administration of Shaofu Zhuyu. *J Chromatogr B Analyt Technol Biomed Life Sci*. 2014; 962: 75-81.
51. Sasaki T, Kinoshita Y, Matsui S, Kakuta S, Yokota-Hashimoto H, Kinoshita K, et al. N-methyl-D-aspartate receptor coagonist D-serine suppresses intake of high-preference food. *Am J Physiol Regul Integr Comp Physiol*. 2015; 309: R561-75.
52. Kolodney G, Dumin E, Safory H, Rosenberg D, Mori H, Radziszewsky I, et al. Nuclear compartmentalization of serine racemase regulates D-serine production: implications for N-methyl-D-aspartate (NMDA) receptor activation. *Journal of Biological Chemistry*. 2016; 291(6): 2630.
53. Madeira C, Lourenco MV, Vargaslopes C, Suemoto CK, Brandão CO, Reis T, et al. D-serine levels in Alzheimer's disease: implications for novel biomarker development. *Transl Psychiatry*. 2015; 5: e561.
54. Lai CH. Sodium benzoate, a D-amino acid oxidase inhibitor, increased volumes of thalamus, amygdala, and brainstem in a drug-naive patient with major depression. *J Neuropsychiatry Clin Neurosci*. 2013; 25: E50-E51.
55. Feng R, Shou JW, Zhao ZX, He CY, Ma C, Huang M, et al. Transforming berberine into its intestine-absorbable form by the gut microbiota. *Sci Rep*. 2015; 5: 12155.
56. Albenberg LG, Wu GD. Diet and the intestinal microbiome: associations, functions, and implications for health and disease. *Gastroenterology*. 2014; 146: 1564-72.
57. Cox LM, Yamanishi S, Sohn J, Alekseyenko AV, Leung JM, Cho I, et al. Altering the intestinal microbiota during a critical developmental window has lasting metabolic consequences. *Cell*. 2014; 158: 705-21.
58. Sekirov I, Russell SL, Antunes LCM, Finlay BB. Gut microbiota in health and disease. *Physiol Rev*. 2010; 90: 859-904.
59. Wang Y, Tong Q, Shou JW, Zhao ZX, Li XY, Zhang XF, et al. Gut microbiota-mediated personalized treatment of hyperlipidemia using berberine. *Theranostics*. 2017; 7: 2443-51.